

# Measuring the yield of singlet oxygen in a chemical oxygen iodine laser (Postprint)

Kevin B. Hewett et al.

01 August 2006

Conference Proceedings

APPROVED FOR PUBLIC RELEASE; DISTRIBUTION IS UNLIMITED.



**AIR FORCE RESEARCH LABORATORY**  
**Directed Energy Directorate**  
**3550 Aberdeen Ave SE**  
**AIR FORCE MATERIEL COMMAND**  
**KIRTLAND AIR FORCE BASE, NM 87117-5776**

## NOTICE AND SIGNATURE PAGE

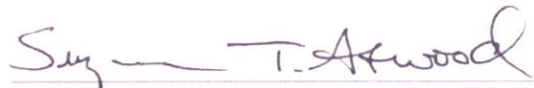
Using Government drawings, specifications, or other data included in this document for any purpose other than Government procurement does not in any way obligate the U.S. Government. The fact that the Government formulated or supplied the drawings, specifications, or other data does not license the holder or any other person or corporation; or convey any rights or permission to manufacture, use, or sell any patented invention that may relate to them.

This report was cleared for public release by the Office of Public Affair, 377th ABW, for the Air Force Research Laboratory, Phillips Research Site, and is available to the general public, including foreign nationals. Copies may be obtained from the Defense Technical Information Center (<http://www.dtic.mil>).

AFRL-RD-PS-TP-2008-1002 HAS BEEN REVIEWED AND IS APPROVED FOR PUBLICATION IN ACCORDANCE WITH ASSIGNED DISTRIBUTION STATEMENT.



KEVIN B. HEWETT, DR-III  
Project Officer



SUZANNE T. ATWOOD, DR-IV  
Acting Chief, Laser Division

This report is published in the interest of scientific and technical information exchange, and its publication does not constitute the Government's approval or disapproval of its ideas or findings.

# REPORT DOCUMENTATION PAGE

*Form Approved*  
OMB No. 0704-0188

Public reporting burden for this collection of information is estimated to average 1 hour per response, including the time for reviewing instructions, searching existing data sources, gathering and maintaining the data needed, and completing and reviewing this collection of information. Send comments regarding this burden estimate or any other aspect of this collection of information, including suggestions for reducing this burden to Department of Defense, Washington Headquarters Services, Directorate for Information Operations and Reports (0704-0188), 1215 Jefferson Davis Highway, Suite 1204, Arlington, VA 22202-4302. Respondents should be aware that notwithstanding any other provision of law, no person shall be subject to any penalty for failing to comply with a collection of information if it does not display a currently valid OMB control number. **PLEASE DO NOT RETURN YOUR FORM TO THE ABOVE ADDRESS.**

<b>1. REPORT DATE</b> (DD-MM-YYYY) 01 Aug 2006		<b>2. REPORT TYPE</b> Conference Proceedings		<b>3. DATES COVERED</b> (From - To) 1 Oct 2004-1 Aug 2006	
<b>4. TITLE AND SUBTITLE</b> Measuring the yield of singlet oxygen in a chemical oxygen iodine laser (Postprint)				<b>5a. CONTRACT NUMBER</b> In-house (DF297833)	
				<b>5b. GRANT NUMBER</b>	
				<b>5c. PROGRAM ELEMENT NUMBER</b>	
<b>6. AUTHOR(S)</b> Kevin B. Hewett, John E. McCord Manish Gupta*, and Thomas Owano*				<b>5d. PROJECT NUMBER</b> MDA6	
				<b>5e. TASK NUMBER</b> LB	
				<b>5f. WORK UNIT NUMBER</b> 02	
<b>7. PERFORMING ORGANIZATION NAME(S) AND ADDRESS(ES)</b> AFRL/RDLC 3550 Aberdeen Ave. SE Kirtland AFB, NM 87117-5776				<b>8. PERFORMING ORGANIZATION REPORT NUMBER</b>	
<b>9. SPONSORING / MONITORING AGENCY NAME(S) AND ADDRESS(ES)</b> Air Force Research Laboratory/RDLC 3550 Aberdeen Ave. SE Kirtland AFB, NM 87117-5776				<b>10. SPONSOR/MONITOR'S ACRONYM(S)</b> AFRL/RDLC	
				<b>11. SPONSOR/MONITOR'S REPORT NUMBER(S)</b> AFRL-RD-PS-TP-2008-1002	
<b>12. DISTRIBUTION / AVAILABILITY STATEMENT</b> Approved for public release; distribution is unlimited					
<b>13. SUPPLEMENTARY NOTES</b> *Los Gatos Research, 67 East Evelyn Ave., Suite 3, Mountain View, CA 94041-1518  Published in XVI International Symposium on Gas Flow, Chemical Lasers, and High-Power Lasers, Proceedings of SPIE, (2007), 6346, 63460E-1, SPIE.  Government Purpose Rights					
<b>14. ABSTRACT</b> A critical parameter for understanding the performance of Chemical Oxygen Iodine Lasers is the yield of singlet oxygen produced by the generator. Off-Axis Integrated Cavity Output Spectroscopy (Off-Axis ICOS) has been utilized to measure the absolute density of both ground-state and singlet oxygen in the cavity of a COIL laser.					
<b>15. SUBJECT TERMS</b> COIL Laser Singlet Oxygen Yield					
<b>16. SECURITY CLASSIFICATION OF:</b>			<b>17. LIMITATION OF ABSTRACT</b>	<b>18. NUMBER OF PAGES</b>	<b>19a. NAME OF RESPONSIBLE PERSON</b>
<b>a. REPORT</b>	<b>b. ABSTRACT</b>	<b>c. THIS PAGE</b>			Kevin B. Hewett
Unclassified	Unclassified	Unclassified	SAR	11	<b>19b. TELEPHONE NUMBER</b> (include area code) 505-853-2684

# Measuring the yield of singlet oxygen in a chemical oxygen iodine laser

Kevin B. Hewett<sup>a</sup>, John E. McCord<sup>a</sup>, Manish Gupta<sup>b</sup>, and Thomas Owano<sup>b</sup>

<sup>a</sup>Air Force Research Laboratory, Directed Energy Directorate, High Power Gas Lasers Branch,  
3550 Aberdeen Ave SE, Kirtland AFB, NM 87117-5776

<sup>b</sup>Los Gatos Research, 67 East Evelyn Avenue, Suite 3, Mountain View, CA 94041-1518

## ABSTRACT

A critical parameter for understanding the performance of Chemical Oxygen Iodine Lasers is the yield of singlet oxygen produced by the generator. Off-Axis Integrated Cavity Output Spectroscopy (Off-Axis ICOS) has been utilized to measure the absolute density of both ground-state and singlet oxygen in the cavity of a COIL laser.

**Keywords:** COIL Laser, Singlet Oxygen Yield

## 1. INTRODUCTION

The Chemical Oxygen Iodine Laser (COIL) is based upon the energy transfer from singlet oxygen to iodine atoms. The reaction kinetics in COIL are complex. Extensive kinetic modeling has shown that a myriad of different reactions are involved including  $O_2(a^1\Delta_g)$  self-quenching,  $O_2(a^1\Sigma_g)$  dissociation of  $I_2$ , and  $O_2(a^1\Delta_g)$  deactivation by  $O_2(X^3\Sigma_g)$  to name a few. Despite these calculations, a substantial amount of chemical energy is still unaccounted for and accurate, quantitative diagnostic measurements are required. These measurement needs are further extended to Electronic Oxygen-Iodine Lasers (EOILs) in which  $O_2(a^1\Sigma_g)$  is generated via an electric discharge. In these devices the kinetics are further complicated by the presence of reactive O atoms. Due to the importance of measuring these species in COIL flows, several techniques have been developed over the past 40 years.

The first COIL diagnostics involved using emission spectroscopy to determine the concentrations of  $O_2(a^1\Delta_g)$  and  $O_2(b^1\Sigma_g)$  by measuring spontaneous emission at 1315 nm and 760 nm respectively<sup>1</sup>. This technique is inadequate for quantification in COIL applications because it is insufficiently accurate (providing densities to only about  $\pm 40\%$ ), requires frequent calibration, provides little internal state information, and is difficult to implement in a complex, lasing media. A significant improvement was realized when tunable diode laser absorption spectrometry was indirectly used to quantify  $O_2(a^1\Delta_g)$  by measuring  $O_2(b^1\Sigma_g)$  and assuming a total concentration of oxygen<sup>2</sup>. However the technique requires well-balanced pathlengths to obviate the effects of atmospheric oxygen and has been difficult to implement in actual COIL devices.

Gyls and Rubin employed spontaneous Raman imaging to measure both  $O_2(a^1\Delta_g)$  and  $O_2(X^3\Sigma_g)$  in a COIL diagnostic duct<sup>3</sup>. Although this technique appears promising, it employs extensive hardware and still requires substantial refinement to be effective. In particular, it cannot provide internal state information, only gives remedial accuracy, and is ineffective in the presence of interfering iodine molecules (as is commonly found in COIL).

In this study, we present data demonstrating the utility of a new COIL diagnostic technique termed Off-Axis Integrated Output Spectroscopy (Off-Axis ICOS). Off-Axis ICOS relies on using a high-finesse optical cavity (typical  $R > 99.99\%$ ) to provide extraordinarily long effective pathlengths ( $L_{\text{eff}} \sim 10$  km) for absorption spectrometry, enabling the accurate quantification of weakly absorbing species<sup>4</sup>. Laboratory results are presented that demonstrate how the technique can be effectively exploited to quantify the electronic state distribution of oxygen in the COIL and EOIL. Additionally, *in-situ* measurements of  $O_2(X^3\Sigma_g)$  on a COIL laser using the Off-Axis ICOS technique are shown., and preliminary data on the reproducibility of singlet oxygen production and associated parameters are discussed. Possible future experiments on the extension of Off-Axis ICOS in the COIL platform are also presented, including direct measurements of the rotational distribution of oxygen, quantifying other key chemical species (e.g.  $I_2$ ,  $H_2O$ , etc...), and applying the diagnostic to the EOIL.

## 2. METHODOLOGY

In standard absorption spectroscopy, a light source is passed through an absorbing sample. The intensity of the light is measured before,  $I_0$ , and after,  $I$ , passage through the sample, and the concentration of the absorbing species can be determined from Beer's Law. Absorption spectroscopy is an attractive analytical tool because it provides an absolute concentration without calibration. However, if the probed species absorbs too weakly (e.g. low concentration or small absorption cross section), the change in transmitted intensity becomes virtually undetectable. The most common solution to this problem is to replace the windows with mirrors and reflect the light back and forth several times (e.g. 33 – 100 typical) through the sample. Despite this enhancement in pathlength, very weak absorbers can still not be detected with sufficient signal-to-noise. Furthermore, these systems are very sensitive to alignment, with even slight beam steering resulting in a large decrease in transmitted power.

### 2.1. Measurement technique

The Off-Axis ICOS technique represents a very simple solution to this problem. Instead of inserting and collecting the beam through holes in the mirrors, the beam enters the gas cell by passing through the input mirror and is collected as it passes through the output mirror as depicted in Figure 1. Light entering the optical cavity bounces back and forth many times tracing out an effective pathlength that is given by the mirror reflectivity. By using highly reflective mirrors ( $R > 99.99\%$ ), the light travels  $>10,000$  passes, providing a significant improvement over multi-pass instruments. By employing an off-axis alignment scheme, the light does not interfere strongly with itself in the cavity, allowing very small changes in intensity to be measured while retaining extraordinarily long pathlengths.

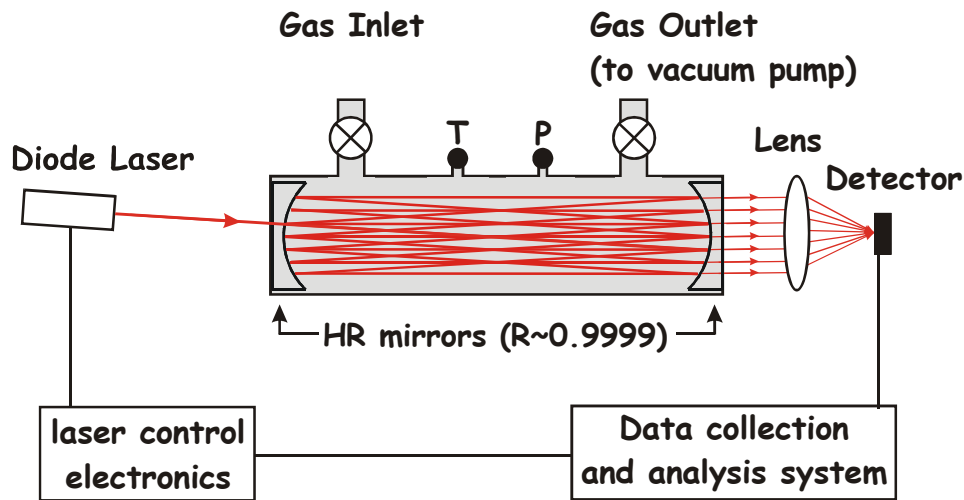


**Fig. 1.** The Off-Axis Integrated Cavity Output Spectroscopy (Off-Axis ICOS) measurement scheme.

Besides its extremely high sensitivity, Off-Axis ICOS is also inherently robust and self-calibrating. Since the pathlength only depends on losses in the cavity and not on the exact beam alignment, it is not necessary to stringently align the optical cavity or the input beam. This allows the Off-Axis ICOS technique to tolerate a very high degree of mechanical vibration and promotes its use as a field instrument. Moreover, the technique becomes self-calibrating by rapidly switching the laser off and measuring the decay of light out of the cavity, similar to the well-established technique of cavity ringdown spectroscopy, but without dithering either the laser or cavity to hit a specific resonance or the “mode-matching” the beam. Due to the robustness and sensitivity of the Off-Axis ICOS technology, it has been routinely used to measure absorptions as small as  $10^{-10} \text{ cm}^{-1}$  and has been applied to a variety of industrial and environmental problems.

## 2.2. Measurement strategy

Off-Axis ICOS can be used to measure the absolute densities of  $O_2(X^3\Sigma_g^-)$ ,  $O_2(a^1\Delta_g)$ , and  $O_2(b^1\Sigma_g)$  in specific rovibrational states. The probed transitions are shown in Figure 2 and their value to COIL/EOIL diagnostics are described below.

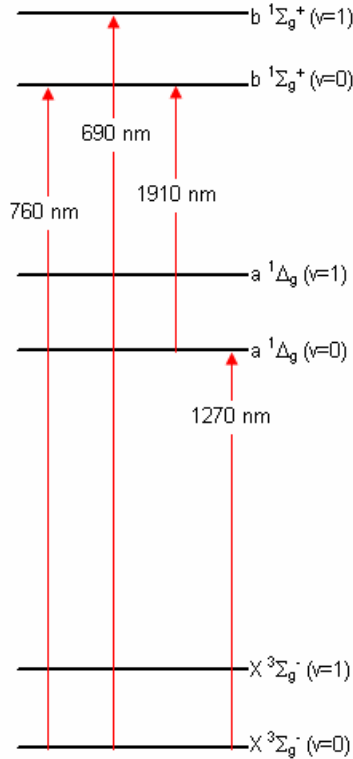


**Fig. 2.** Energy level diagram of the first three electronic states of oxygen. Also shown are the transitions used in this work.

### 3.1.1. $O_2(X^3\Sigma_g^-)$

The absolute density of  $O_2(X^3\Sigma_g^-)$  is probed by measuring the  $O_2(b^1\Sigma_g)$  [ $v=0$ ]  $\leftarrow$   $O_2(X^3\Sigma_g^-)$  [ $v=0$ ] transition near 760 nm. In standard COIL, the  $O_2(b^1\Sigma_g)$  population is expected to be virtually nonexistent (with the exception of a small contribution from  $O_2(a^1\Delta_g)$  recombination) due to quenching by water vapor. In EOIL, there is no water vapor and researchers expect substantially more  $O_2(b^1\Sigma_g)$ . However, models suggest that the  $O_2(b^1\Sigma_g)$  density slightly downstream of the discharge nozzle is still  $< 1\%$  of the  $O_2(X^3\Sigma_g^-)$  density. Therefore, the  $O_2(b^1\Sigma_g)$  [ $v=0$ ]  $\leftarrow$   $O_2(X^3\Sigma_g^-)$  [ $v=0$ ] transition will provide a good measure of  $O_2(X^3\Sigma_g^-)$  density in both cases (to within 1%).

### 3.1.2. $O_2(a^1\Delta_g)$

The absolute density of  $O_2(a^1\Delta_g)$  will be probed by measuring the  $O_2(b^1\Sigma_g)$  [ $v=0$ ]  $\leftarrow$   $O_2(a^1\Delta_g)$  [ $v=0$ ] transition near 1910 nm<sup>5</sup>. Additionally, measurements of the  $O_2(a^1\Delta_g)$  [ $v=0$ ]  $\leftarrow$   $O_2(X^3\Sigma_g^-)$  [ $v=0$ ] transition near 1285 nm were made for self-consistency. This measurement, which is directly proportional to the population difference between the  $X^3\Sigma_g^-$  and  $a^1\Delta_g$  states, will be used to confirm the 1910 nm data.

### 3.1.3. $O_2(b^1\Sigma_g)$

Unlike the aforementioned electronic states, the  $b^1\Sigma_g$  state cannot be readily probed via direct absorption due to the lack of an amenable higher electronic state. To overcome this problem, a scheme is employed that involves probing the  $O_2(b^1\Sigma_g)$  [ $v=0$ ]  $\leftarrow$   $O_2(X^3\Sigma_g^-)$  [ $v=0$ ] transition near 760 nm and the  $O_2(b^1\Sigma_g)$  [ $v=1$ ]  $\leftarrow$   $O_2(X^3\Sigma_g^-)$  [ $v=0$ ] transition near 690 nm. If the  $O_2(b^1\Sigma_g)$  [ $v=1$ ] population is considerably smaller than the  $O_2(b^1\Sigma_g)$  [ $v=0$ ] population, the difference between these two absorption measurements will give the  $O_2(b^1\Sigma_g)$  [ $v=0$ ] population. In the traditional COIL, this measurement is of little value due to the presence of water vapor which rapidly quenches  $O_2(b^1\Sigma_g)$ ; however, it is of significant utility in the case of EOIL where there is expected to be significant populations of  $O_2(b^1\Sigma_g)$ .

## 3. RESULTS

Prior to incorporating the ICOS system on a COIL, the measurement strategy was extensively tested by utilizing an absorption cell. Expected sensitivities had been calculated using typical signal-to-noise ratios for the stated concentrations. These sensitivities were empirically determined by emulating the conditions expected in the COIL. Specifically, a 10 cm long cell was filled with  $\sim 6$  Torr of room air to represent the total pressure in a typical COIL laser cavity and the approximate oxygen content (e.g. 1.3 Torr of oxygen). Note that, due to the low measurement pressure, there is very little peak broadening and the exact composition of the background gas is not critical. Measurements were made in this 10 cm system and the signal-to-noise was empirically determined to give a minimum detectable oxygen density for a given measurement time. Once the absorption cell measurements were completed, the ICOS system was installed on a COIL laser. The measurements were performed in the laser cavity during normal laser operation. The results from both sets of measurements are described below.

### 3.1. Gas cell measurements

#### 3.1.1. $O_2(X^3\Sigma_g)$

The  $O_2(b^1\Sigma_g) [v=0, J=8] \leftarrow O_2(X^3\Sigma_g) [v=0, J=9]$  transition near 760 nm was examined in a static cell. A single-sweep measured cavity-enhanced absorption signal obtained in 0.01 seconds (e.g. 100 Hz) is shown in Figure 3 fit to a Voigt profile. Note the very high signal-to-noise per sweep of approximately 80:1 without any data averaging. Note that the detection limit is based upon the number density in a particular ro-vibrational quantum state. The gas phase temperature (corresponding to a Boltzmann distribution) is required to determine a number density of all oxygen in the  $O_2(X^3\Sigma_g)$  state. The detection limit for this transition is shown in Table 1.

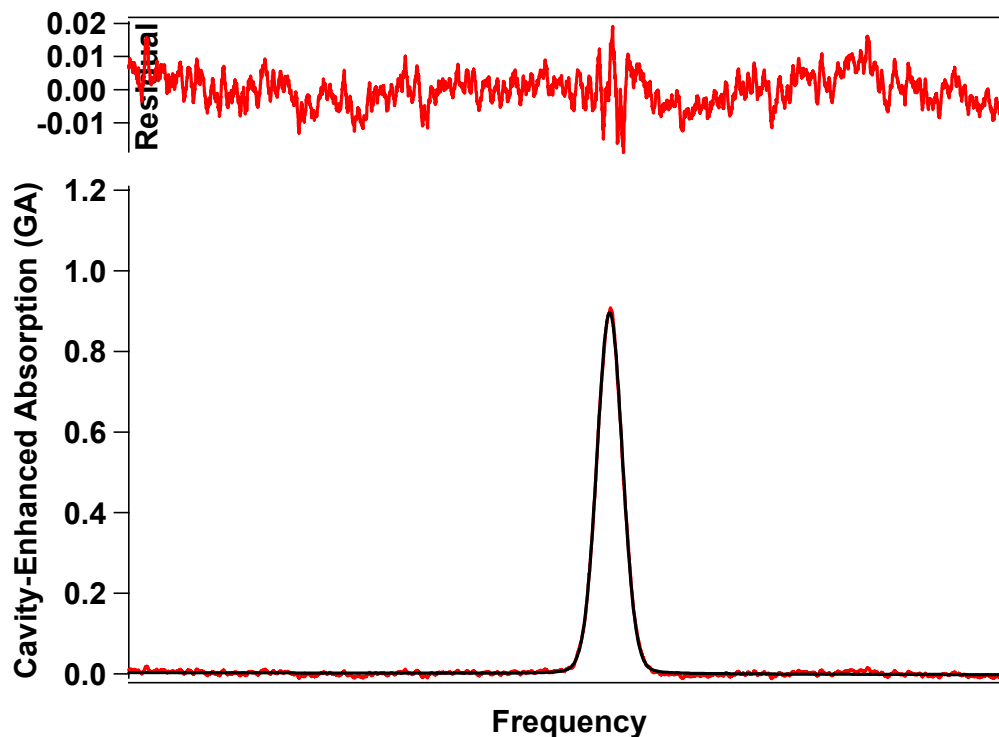


**Fig. 3.** Measured cavity-enhanced absorption signal of the  $O_2(b^1\Sigma_g) [v=0, J=8] \leftarrow O_2(X^3\Sigma_g) [v=0, J=9]$  transition near 763 nm without any data averaging yields a signal-to-noise of approximately 80:1.

**Table 1.** The transitions examined and the detection limits for each at a rate of 2 Hz.

Species	Transition	$\lambda$ (nm)	Detection Limit (per quantum state)
$O_2(X^3\Sigma_g)$	$O_2(b^1\Sigma_g) [v=0, J=8] \leftarrow O_2(X^3\Sigma_g) [v=0, J=9]$	760	$2.8 \times 10^{12}$
$O_2(a^1\Delta_g)$	$O_2(b^1\Sigma_g) [v=0, J=12] \leftarrow O_2(a^1\Delta_g) [v=0, J=12]$	1910	$3.1 \times 10^{13}$
	$O_2(a^1\Delta_g) [v=0, J=13] \leftarrow O_2(X^3\Sigma_g) [v=0, J=14]$	1285	$3.8 \times 10^{14}$
$O_2(b^1\Sigma_g)$	$O_2(b^1\Sigma_g) [v=0, J=6] \leftarrow O_2(X^3\Sigma_g) [v=0, J=7]$	690	$1.3 \times 10^{13}$

#### 3.1.2. $O_2(a^1\Delta_g)$

The results for the  $O_2(b^1\Sigma_g) [v=0] \leftarrow O_2(a^1\Delta_g) [v=0]$  transition near 1910 nm have been detailed previously<sup>5</sup>. Briefly, the ICOS system demonstrated a signal-to-noise ratio of 120:1 and a detection limit of  $3.1 \times 10^{13}$  molecules  $cm^{-3}$  per quantum state (at 2 Hz).

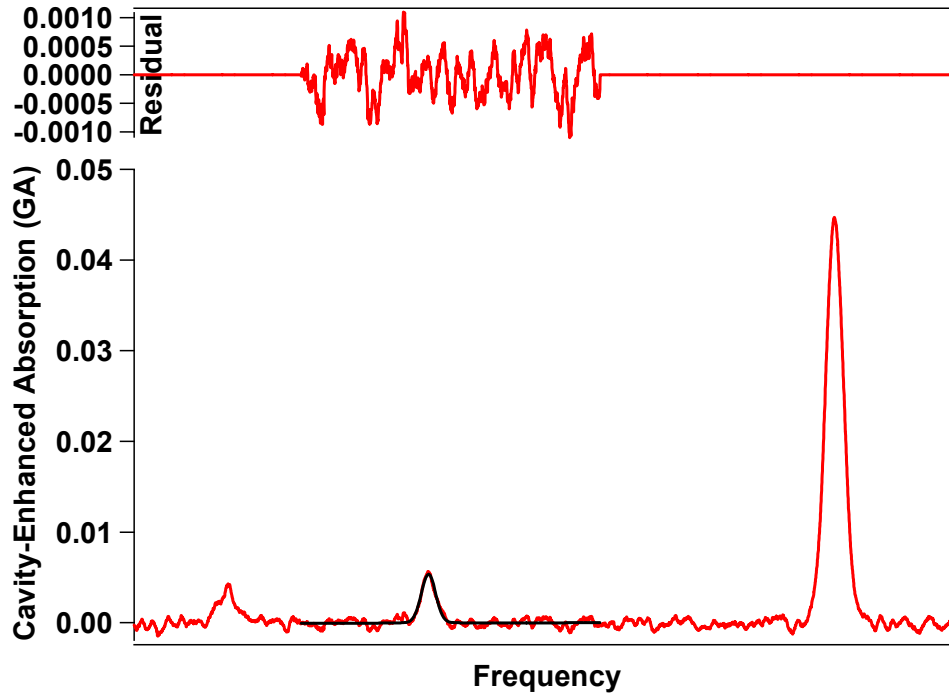


**Fig. 4.** Measured cavity-enhanced absorption signal of the  $O_2(a^1\Delta_g) [v=0] \leftarrow O_2(X^3\Sigma_g) [v = 0]$  transition near 1285 nm after 1 second of data averaging yields a signal-to-noise of approximately 12:1. Note that the other two absorption features in the spectra are due to ambient water vapor.

The  $O_2(a^1\Delta_g) [v=0] \leftarrow O_2(X^3\Sigma_g) [v = 0]$  transition near 1285 nm is very weak even near its bandhead at 1270 nm. Due to the difficulty in obtaining diode lasers at wavelengths shorter than 1285 nm, the absorption transition is even weaker at the operating wavelength. Despite these limitations, Off-Axis ICOS is capable of measuring this transition under the simulated COIL conditions. Note that it requires 1 second of data averaging (100 spectra) to measure this transition with a signal-to-noise of 12:1. The detection limit is shown in Table 1.

### 3.1.3. $O_2(b^1\Sigma_g)$

The single-sweep transmission signal (e.g. 0.01 seconds, 100 Hz) for the oxygen absorption near 690 nm is shown in Figure 5. Note that the absorption is significantly smaller than that near 763 nm and has a signal-to-noise of only 18:1. The minimum detectable density per quantum state is shown in Table 1.

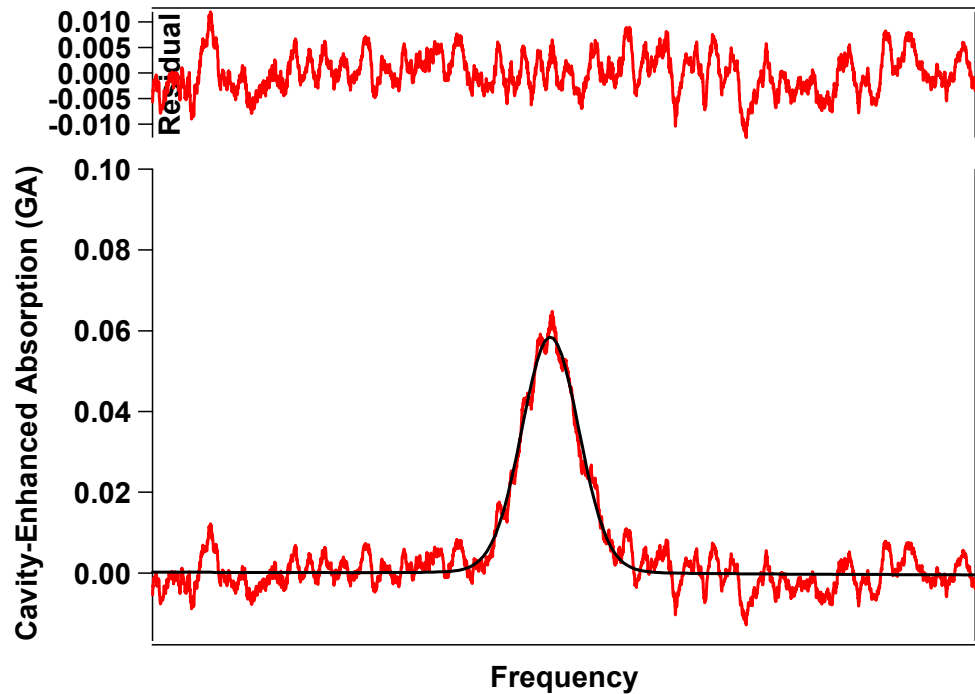


**Fig. 5.** Measured cavity-enhanced absorption spectrum of the  $O_2(b^1\Sigma_g^-) [v = 1] \leftarrow O_2(X^3\Sigma_g^-) [v = 0]$  transition near 690 nm without any data averaging. The signal-to-noise is approximately 18:1.

### 3.2. COIL measurements

In order to demonstrate the utility of the Off-Axis ICOS technique on an actual COIL, the system was integrated into a test stand at the Air Force Research Laboratory (Kirtland Air Force Base, Albuquerque, NM). The ICOS mirror mounts were installed on the cavity of the laser with the optical axis located approximately 10 cm downstream of the nozzle exit plane. The mirrors and laser designed for the  $O_2(b^1\Sigma_g^-) [v = 0, J = 8] \leftarrow O_2(X^3\Sigma_g^-) [v = 0, J = 9]$  transition near 763 nm was installed and the COIL was repeatedly fired. The measured density of  $O_2(X^3\Sigma_g^-) [v = 0, J = 9]$  is shown in Figure 6 for three consecutive firings. In the absence of chlorine, the diagnostic detects the residual oxygen in the laser system. When chlorine is added, the BHP + chlorine reaction forms both ground and singlet state oxygen. The water vapor produced immediately quenches any  $O_2(b^1\Sigma_g^-)$ , making the diagnostic a direct measure of the number density in the  $O_2(X^3\Sigma_g^-) [v = 0, J = 9]$  quantum state. The results shown in Figure 6 clearly indicate that a large density of ground-state oxygen is produced.

The process of turning the measured quantum state number density into a  $O_2(a^1\Delta)$  yield is non-trivial. The yield is defined as the ratio of  $O_2(a^1\Delta)$  to total  $O_2$ . The total amount of oxygen produced is determined from the chlorine flow and the chlorine utilization. This assumes that all oxygen produced enters into the laser cavity. Due to the rapid quenching of any  $O_2(b^1\Sigma_g^-)$  by water, it can be assumed that the  $O_2(\text{total}) = O_2(a^1\Delta) + O_2(X^3\Sigma_g^-)$ . The  $O_2(X^3\Sigma_g^-)$  number density is determined by using an estimate of the gas phase temperature to convert the quantum state number density (as measured by Off-Axis ICOS) into a total number density via a thermalized Boltzmann distribution. With the total oxygen and the ground state oxygen number densities, the singlet delta number density is determined by simple subtraction and the yield can then be determined. The major difficulty in making this measurement is obtaining an accurate measurement of the gas phase temperature and future work will focus on extending this technique as noted below.

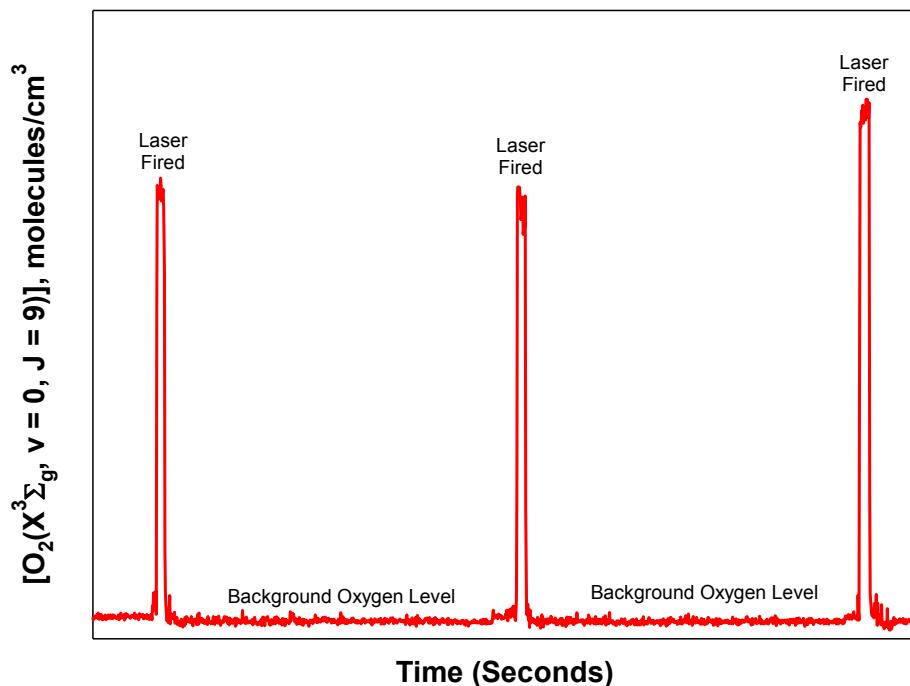


**Fig. 6.** *In Situ* measurements of the oxygen density in a COIL cavity via Off-Axis ICOS. When the laser is fired (i.e. chlorine is turned on) the ground state oxygen number density increases dramatically.

#### 4. CONCLUSIONS AND FUTURE WORK

Measurements of the number density of oxygen have been performed on an operational COIL. These measurements, when combined with the chlorine flow rate and chlorine utilization data will allow for a yield of singlet oxygen to be measured. Ongoing work will enable researchers at AFRL and Los Gatos Research to more accurately measure the yield as additional measurements are performed. Future efforts will include measuring the  $O_2(b^1\Sigma_g) [v=0] \leftarrow O_2(a^1\Delta_g) [v=0]$  transition near 1910 nm for a direct  $O_2(a^1\Delta_g)$  quantification as well as modifying the Off-Axis ICOS system to measure the number density in multiple quantum states (and thus measure the rotational temperature directly). Further studies will involve extending the analysis to other small molecules of chemical interest including water, iodine, and nitric oxide (for EOIL applications).

#### 5. ACKNOWLEDGEMENTS

The authors would like to thank Dr. David Hostutler, Mr. Chris Cooper and SSgt. Ransom Oswald for their help in reconfiguring the COIL test stand to accept the ICOS instrument.

#### REFERENCES

- <sup>1</sup> S. J. Arnold, N. Finlayson, and E. A. Ogryzlo, *J. Chem. Phys.*, **44**, 2529 (1966).
- <sup>2</sup> S. J. Davis, M. G. Allen, W. J. Kessler, K. R. McManus, M. F. Miller, and P. A. Mulhall, *OE-Lase Conf. SPIE Paper*, **2702-17** (1996).
- <sup>3</sup> V. T. Gylys and L. F. Rubin, *Appl. Opt.*, **37**, 1026 (1998).
- <sup>4</sup> D.S. Baer, J.B. Paul, M. Gupta, and A. O'Keefe, *Applied Physics B, Lasers and Optics* **75**, 261-265 (2002).
- <sup>5</sup> M. Gupta et al., *Chem. Phys. Lett.* **400**, 42 (2004).

## DISTRIBUTION LIST

DTIC/OCP

8725 John J. Kingman Rd, Suite 0944

Ft Belvoir, VA 22060-6218

1 cy

AFRL/RVIL

Kirtland AFB, NM 87117-5776

2 cys

Official Record Copy

AFRL/RDLC/Kevin B. Hewett

1 cy